JOURNAL OF PHYSICAL ORGANIC CHEMISTRY
J. Phys. Org. Chem. 2005; **18:** 26–34
DOI: 10.1002/poc.808

Geometry and binding properties of different multiple-state glycine–Fe^+/Fe^{2+} complexes

Hongqi Ai,[1] Yuxiang Bu,[1,2,3]* Ping Li,[1] Zhiqiang Li,[1] Xiangquan Hu[2] and Zhida Chen[2]

[1]Institute of Theoretical Chemistry, Shandong University, Jinan 250100, China
[2]State Key Laboratory of Rare-Earth Materials and their Application, Peking University, Beijing 800871, China
[3]Department of Chemistry, Qufu Normal University, Qufu 273165, China

Received 3 June 2003; revised 15 October 2003; accepted 18 March 2004

ABSTRACT: Several biologically relevant glycine–Fe^+/Fe^{2+} complexes with three different multiplicities were studied for the first time by using the hybrid three-parameter B3LYP density functional method with different basis sets. Single-point calculations were also carried out at the BHLYP level with a larger basis set to refine and calibrate these energy values. The results show that the most stable glycine–Fe^+ isomer is the C_1-symmetric sextet **NO-16**, in which Fe^+ is interacted with both the amino nitrogen and carbonyl oxygen of the glycine ligand. The ground-state structure of glycine–Fe^{2+} is the $^5A''$ state **2O-25**, which generates from the interaction of Fe^{2+} with the two oxygen terminus of the zwitterionic glycine. The calculations indicate that the binding energies mainly derive from the contributions of electrostatic effects, for both the monovalent and divalent metal cation-chelated glycine complexes. The differences in binding energies between these different multiple-state glycine–Fe^+ isomers with same combination modes mainly derive from their different electrostatic and polarized effects, and those between the isomers of different combination modes with the same multiple states mainly stem from their different deformation effects. The differences in the relative stabilities of these glycine–Fe^+ isomers with different multiple states mainly come from the fact that the more electrostatic contribution of the lower spin complex cannot compensate for the loss of energy enhancement of its corresponding metal cation relative to that of the higher spin counterpart. The same is true for the glycine–Fe^{2+} complexes.

KEYWORDS: DFT calculations; glycine–Fe^+/Fe^{2+} complexes; structures; relative energies; binding energies; binding energy analysis

INTRODUCTION

The study of the interaction between a transition metal cation and a glycine is an area of intense interest owing to the importance of such interactions in life processes. The cations involved with similar interactions include Ag^+, Ni^+, $Cu^{+/2+}$ and $Zn^{+/2+}$.[1–8] However, prior to this work, there have not been any reports of the application of density functional theory (DFT) to or other calculations on the interactions of a glycine and iron cations except those on the interactions between an iron cation and some small ligands, such as H_2O[9] and NH_3,[10] maybe owing to the computational complexity of glycine–iron cation systems.

Iron cations are very important and indispensable materials in biological systems; the Fe cations in biological systems are usually divalent or trivalent and the coordination sphere is saturated. For example, the coordination number at the active centers of enzymes is six in most cases. This indicates that, in a real biological system, less than one charge distribution of, for example, a trivalent Fe cation contributes to the interaction with an active site of a biological molecule. Hence both monovalent and divalent Fe cations as models are employed to investigate the interactions with biological molecules. Nitrogen and oxygen atoms in amino acids, peptides or proteins are the main active sites, and glycine is the simplest of the 20 common amino acids and holds the basic characteristics of the others. Considering its ease of manipulation in computations relative to other amino acids, glycine would be a suitable model for the investigation of interactions with Fe^+/Fe^{2+} by using accurate computational methods of quantum chemistry. A glycine molecule has three different active sites, i.e. the amino nitrogen (N3), hydrogen oxygen (O4) and carbonyl oxygen (O5) sites. One or even both neighboring active sites can bind with an Fe^+/Fe^{2+} cation. Various studies[1–7] had concluded that the most stable combination modes for a transition metal cation and glycine should not go beyond two ones, i.e. the cation bound to both the N3 and O5 sites of the neutral glycine or to both oxygen ends of the zwitterionic glycine [see Fig. 1(I) and (II)]. A special

---

**Correspondence to:* Y.-X. Bu, Institute of Theoretical Chemistry, Shandong University, Jinan 250100, China.
E-mail: byx@sdu.edu.cn
Contract/grant sponsor: National Natural Science Foundation of China; *Contract/grant number:* 20273040.
Contract/grant sponsor: Natural Science Foundation of Shandong Province; *Contract/grant number:* Z2003B01.
Contract/grant sponsor: SRFDP.

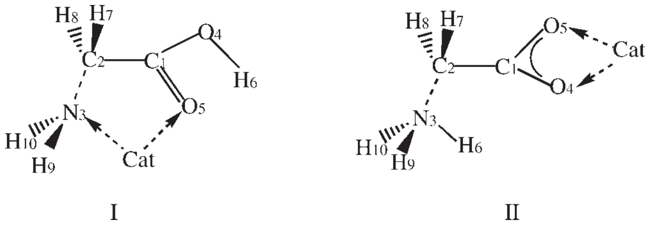

Figure 1. Two selected stable combination modes for glycine and cation (Cat) (Fe^{+}/Fe^{2+})

study on the combination modes by Hoyau *et al.*[11] also confirmed this.

Fe^{+} has five unpaired electrons in its outer shell orbitals, which corresponds to a multiplicity of 2, 4 or 6. Therefore, the corresponding multiplicity is also 2, 4 or 6 for the Fe^{+}-bound glycine molecule. Similarly to Fe^{+}, the multiplicities for the Fe^{2+}-bound complexes may be 1, 3 or 5. Hence there should be six different coupling cases when Fe^{+}/Fe^{2+} interacts with a glycine molecule. Including the two most stable combination modes mentioned above, 12 complexes can be obtained. Owing to the many unpaired electrons and multiplicities in an Fe^{+}/Fe^{2+} cation, too much computational time is necessary to elucidate these complexes. Fortunately, we have finally obtained the optimized complexes. The major aim of this work was to probe the interaction of an Fe^{+}/Fe^{2+} cation with two selected glycine molecules and to provide some valuable information for the study in the fields of catalysis, atmospheric chemistry and biochemistry. The effects of different valence states and multiplicities on the geometries, stabilities and binding energies of these iron cation-chelated glycine complexes represent a very interesting unknown field which motivated us to make a detailed examination.

COMPUTATIONAL METHODS

The combination of Becke's three-parameter hybrid exchange functional[12] with the Lee, Yang and Parr (LYP) correction[13] (B3LYP) functional of the DFT method have successfully dealt with many transition metal cation-chelated glycine systems.[1,3–8] Recent studies on the conformational behavior of glycine and other amino acids[14–16] had also shown that the B3LYP method could provide structural parameters that were very similar those obtained by the MP2 method[17] and the vibrational frequencies and intensities were in excellent agreement with the experimental data.[1] Hence full geometry optimization, natural orbital analysis and harmonic vibrational frequency calculations were performed with the same method.

The geometry optimizations and the corresponding frequency calculations for these complexes have employed the 6–31G* basis set (basis1).[18] Larger basis sets, 6–31+G* (basis2)[19] and 6–311+G* (basis3),[20] have also been used in single-point calculations so that the effects of diffusion and larger basis set are taken into account. Owing to the possibly greater reliability of basis3, the calculations on the relative energies included unscaled zero point vibrational energy (ZPVE) correction of basis1-optimized frequencies, and the energies of the metal iron cations were treated with this basis set.

It is known that DFT methods tend to overstabilize d^{n+1} occupations versus $d^{n}s^{1}$ occupations. For example, Baerends *et al.*[21] reported that DFT calculations would lead to uncertainties of 3–5 kcal mol^{-1} (1 kcal = 4.184 kJ) in the atomic ground state energy of the transition metal elements. B3LYP/basis2/3 methods also showed the quartet state to be the most stable in our present calculations. Such errors can carry over to the complex in such a way that the calculations for glycine–Fe^{+} complexes are artificially biased toward the quartet state. Hence this is particularly problematic for Fe^{+} because its electronic ground state is the $3d^{6}4s^{1}$ (^{6}D) state, whereas the d^{7} (^{4}F) state lies 0.25 eV above. All these factors imply that it is of importance to investigate the reliability of energies obtained at the B3LYP level and to calibrate these values. Therefore, the *ab initio* methods MP2(full)/basis1–3 and the CCSD(T)/6–311++G(2d,2p)(CCSD(T)/basis4)[22] method were also employed for calculations on the different valent-state Fe^{+}/Fe^{2+} cations. The admixture of exact exchange reduces the error and the DFT approach that is better than post-Hartree–Fock calculations is the BHLYP method,[23] for which the mixing is 50%.[1,24] Moreover, the BHLYP calculations can save considerable time relative to post-Hartree–Fock calculations for the treatment of a complex system, so the BHLYP was also used in this work for greater accuracy and efficiency. The calculations in the following sections showed that this method can offer relatively ideal results for treating glycine–Fe^{+}/Fe^{2+} systems, so the binding energies, electrostatic effects and deformation energy calculations of these systems were investigated with this method and basis4. Basis set superposition error (BSSE)[25] corrections were considered in the binding energy calculations.

In order to gain further insight into the binding cases for each individual system, we will discuss it in detail in several separate respect,[2,26] as proposed by Kitaura and Morokuma[27] and Glendening and Streitwieser:[28]

$$\Delta E = \Delta E_{\mathrm{e}} + \Delta E_{\mathrm{p}} + \Delta E_{\mathrm{ct}} + \Delta E_{\mathrm{r}} + \Delta E_{\mathrm{d}} + \mathrm{BSSE} \quad (1)$$

where ΔE_{e} denotes the electrostatic energy contribution, i.e. the energy lowering of the deformed glycine in the presence of a single (or two) point charge(s) at the same glycine distance. As the electrostatic relaxation of glycine was allowed, the actual lowering (listed in Table 4) also includes the polarization term (ΔE_{p}). ΔE_{ct} is the charge-transfer term, ΔE_{r} is the short-range repulsion energy, calculated as the sum of bond–bond, bond–lone pair and lone pair–lone pair interactions and ΔE_{d} denotes the deformation energy term obtained from the difference between glycine at the geometry of the complex and

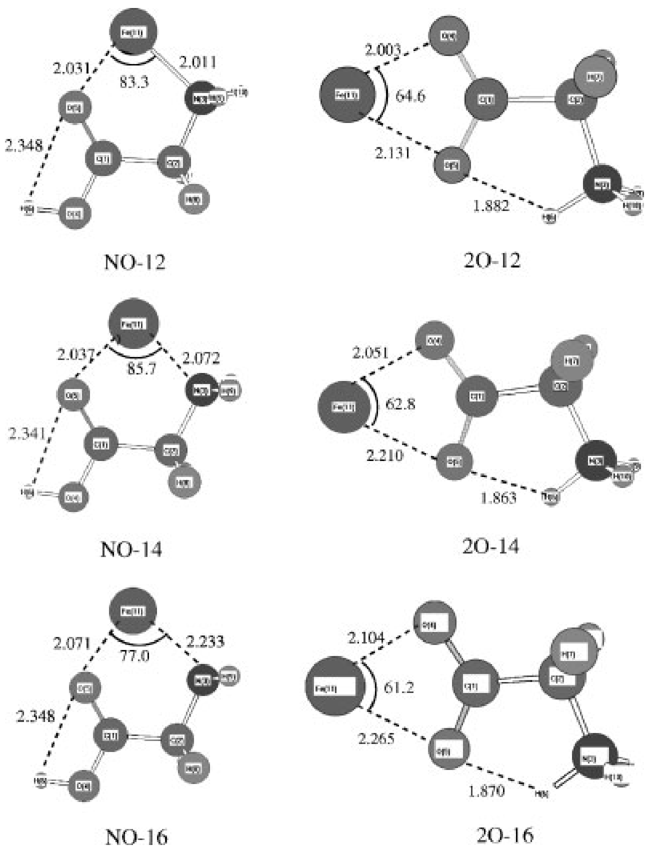

Figure 2. B3LYP/basis1-optimized glycine–Fe$^+$ isomers. Distances in ångstroms and angles in degree

the free glycine in its ground-state structure. Among these terms, the first three contributions favor the stability of the complex and the last two destabilize the complex.

All these calculations were performed using the Gaussian 98 package of programs, version A.9.[29]

RESULTS AND DISCUSSION

Relative stability and geometries of six glycine–Fe$^+$ isomers

Figure 2 shows the geometries of six glycine–Fe$^+$ isomers, denoted **NO-1n** and **2O-1n** (**n** = **2**, **4** or **6**). **NO** denotes the combination of monovalent iron (Fe$^+$) chelated by both the amino nitrogen (N3) and carbonyl oxygen (O5) sites of the neutral glycine and **2O** stands for the Fe$^+$ bound by both carbonyl oxygen (O5) and hydrogen oxygen (O4) of the zwitterionic glycine. The number **1** in **1n** denotes the valence of Fe and **n** denotes the corresponding spin multiplicity. Hence for Fe$^+$ with many unpaired electrons in its 3d4s orbitals, three corresponding occupied modes of electron are taken into account, corresponding to multiplicities of 2, 4 and 6.

For these Fe$^+$-chelated glycine complexes, the optimizations are performed without any symmetry by rotating the iron cation 5–10° out of the symmetric plane of the five heavy atoms of the glycine. Additional trial structures are generated by rotation dihedral angles selected by chemical intuition. The optimizations show that all these glycine–Fe$^+$ isomers are C_1-symmetric structures, but with six heavy atoms in almost a plane. Frequency calculations reveal that all of these isomers are genuine minima (i.e. having no imaginary frequencies).

Table 1 lists the relative energies of the six isomers. The results show that all the different calculation methods give reasonable agreement for the relative stability of these complexes except for the quartet and sextet state complexes. In detail, the B3LYP method with basis1 shows that the ground-state glycine–Fe$^+$ should be the **NO-16**, which is in agreement with the ordering of the relative stability of their corresponding metal ion with same spin states. However, single-point calculations with larger basis sets (basis2 and basis3) show that **NO-14** is the ground-state complex. The conflicting results derived from the basis set effects are also observed in the **2O** mode counterparts. Hence for these problematic results, detailed investigations are of great importance. Maybe the error cases stemming from the level or basis set expected above really occur. Now we will probe the problem with different levels and basis sets by employing the iron cation with different spin states.

Table 2 gives the relative energies of the three different spin-state iron cations (Fe$^+$/Fe^{2+}) obtained at different levels and with different basis sets. We can observe that the MP2(full) method with three different basis sets offers a very consistent ordering of the relative stability of the three different spin-state monovalent iron ion. Calculated $\langle S^2 \rangle$ values with the three different basis sets for the most stable doublet and quartet state Fe cations after removing the spin contamination are 3.75 and 8.75, respectively, also indicating good reliability. The obtained ordering of their relative energies is also in agreement with the experimental results although these relative values are somewhat overestimated by the

Table 1. Relative energies (kcal mol^{-1}) of glycine-Fe$^+$ isomers obtained at the different levels[a]

Level	NO-16	NO-14	2O-16	2O-14	NO-12	2O-12
B3LYP/basis1	0.0(52.0)	5.0(51.9)	4.4(52.2)	8.3(52.1)	30.4(52.2)	37.0(52.3)
B3LYP/basis2//B3LYP/basis1	0.0	−9.7	−10.1	−3.3	27.1	39.8
B3LYP/basis3//B3LYP/basis1	0.0	−4.1	3.1	−3.4	20.1	31.0
BHLYP/basis4//B3LYP/basis1	0.0	1.6	18.2	18.9	28.9	46.8

[a] Values in parentheses are the ZPVEs of the corresponding complexes. The results in rows 3 and 4 are corrected with the ZPVEs.

Table 2. Relative energies (kcal mol^{-1}) of the three different spin state Fe$^+$/Fe^{2+} obtained at different levels and basis sets

Method	Fe-16	Fe-14	Fe-12	Fe-25	Fe-23	Fe-21
B3LYP/basis1	0.0	15.0	52.4	0.0	58.3	123.4
B3LYP/basis2	0.0	−2.2	24.3			
B3LYP/basis3	0.0	−4.7	21.8	0.0	57.4	120.4
MP2(full)/basis1	0.0	72.1	159.1			
MP2(full)/basis2	0.0	26.8	158.1			
MP2(full)/basis3	0.0	21.0	155.9			
BHLYP/basis4	0.0	3.7	34.0	0.0	41.9	96.7
CCSD(T)/basis4	0.0	5.9	−14.7	0.0	68.2	98.8
MCPF[a]	0.0	9.4	—			
Experimental result[a]	0.0	5.8	44.8[b]			

[a] Results are from Ref. 9.

[b] Energy is from a statistically average.[31]

method. This also occurs with B3LYP/basis1. Surprisingly, B3LYP/basis2/3 markedly underestimates the energies of quartet state Fe$^+$. Table 2 reveals that CCSD(T)/basis4 offers an excellent ^{4}F–^{6}D (Fe$^+$) separation (5.9 kcal mol^{-1}) and the result agree very well with the experimental result [5.8 kcal mol^{-1} (Refs 9 and 10)]. However, the level underestimates the energy of doublet state Fe$^+$, which seriously conflicts with the fact of ^{6}D being the ground state of Fe$^+$. Hence including the expensive cost of CPU time, CCSD(T) is also not the ideal candidate to treat the complex glycine–Fe$^+$ systems. Rosi and Bauschlicher[9] treatment of the separation with the correction using the modified coupled pair functional (MCPF) method followed by a larger basis set provided a 9.4 kcal mol^{-1} energy, which also showed a larger error. Only the BHLYP method with a suitable basis set is the optimum, as verified by its giving results close to the experimental values for the monovalent Fe cation with three different spin states. Also the results obtained at that level are in agreement with those of CCSD(T) for the treatment of the energies of divalent Fe cation with three different spin states. In contrast to Fe$^+$, B3LYP with basis1–3 all give a reasonable ordering for the relative stability of three different spin Fe^{2+} cations. In summary, B3LYP/basis2/3 would give reasonable results for the energies of Fe$^+$(Fe^{2+}) with three different spin states except for the ^{4}F–^{6}D (Fe$^+$) separation. BHLYP/basis4 would be an ideal method to calibrate these errors, which others cannot. Hence the following discussions on these glycine–Fe$^+$/Fe^{2+} complexes are mainly focused on the BHLYP-calibrated results.

As expected, Table 1 shows that the B3LYP method with basis2/3 also provides a ground-state glycine–Fe$^+$ with a quartet not with a sextet state, which is carried over from the errors of the ^{4}F–^{6}D (Fe$^+$) separation obtained at the same level and with the same basis sets.

From Table 1 and Fig. 2, we can observe that the most stable complex is **NO-16**, in which a 2.233 Å N3—Fe bond and 2.071 Å O5—Fe bond are generated. The N3—Fe11—O5 angle is 77.0°. These parameters are very similar to those of the most stable glycine–Cu$^+$ complex reported by Bertran *et al.*[1] The most stable glycine–Zn^{+30} and glycine–Ni^{+6} complexes also show similar bond distances.

The next most stable complex in energy is **NO-14**, in which, just as in **NO-16**, Fe$^+$ is bound to both the carboxyl oxygen and the amino nitrogen of the glycine, with a relative short O5—Fe bond (2.037 Å) and N3—Fe bond (2.072Å). The complex lies only 1.6 kcal mol^{-1} in energy higher than **NO-16**. Single-point calculation at the B3LYP/basis3 level, however, shows that this complex (**NO-14**) is the ground state of its isomers, which indicates the importance of the choice of basis set and methods for calculations on this kind of sensitive system. In comparison with **NO-16**, we can observe that **NO-14** has a more compact structure, which favors its stability. However, the ^{4}F–^{6}D (Fe$^+$) separation (3.7 kcal mol^{-1}) makes its complex energy still higher than the former.

The third most stable complex is **2O-16**, which shows the combination mode II in Fig. 1, in which the Fe cation is bound to both oxygen ends of the zwitterionic glycine. The O4—Fe and O5—Fe bond distances in the complex are 2.104 and 2.265 Å, respectively. Table 1 shows that the complex has energy 18.2 kcal mol^{-1} higher than the ground-state **NO-16**. The higher energy mainly stems from its larger deformation. The phenomenon can also be observed intuitively from Table 3, which gives the charge distribution (Fe$^+$/Fe^{2+}) and the dipole moment of different glycine–Fe$^+$/Fe^{2+} complexes obtained at the B3LYP/basis1 level. Both of the two sextet state glycine–Fe$^+$ complexes have similar charge populations on each Fe cation [0.70 (**2O**) vs 0.65 (**NO**)]. However, the calculated results for the binding energies and its two main contributions listed in Table 4 show that the deformation energy in the **2O** mode is 27.4 kcal mol^{-1} higher than that (7.6 kcal mol^{-1}) in the **NO** mode. The larger electrostatic effect of the former (−89.4 kcal mol^{-1}) relative to the latter (−79.8 kcal mol^{-1}) cannot compensate for its deformation loss, which results in its poorer stability.

The fourth most stable complex is **2O-14** isomer, which shows similar to the corresponding **2O-16** isomer in structure. Table 1 shows that the **2O-14** isomer is energetically higher by 18.9 kcal mol^{-1} than **NO-16** and by 0.7 kcal mol^{-1} than **2O-16**. The O5—Fe and O4—Fe

Table 3. Charge distribution (Fe^+/Fe^{2+}) and the dipole moments of glycine–Fe^+/Fe^{2+} complexes obtained at the B3LYP/basis1 level

	2O-12	**2O-14**	**2O-16**	**NO-12**	**NO-14**	**NO-16**
Fe^+	0.62	0.65	0.70	0.63	0.64	0.65
Dipole moment (D)	8.7	8.5	9.0	2.1	2.7	3.4
	2O-21	**2O-23**	**2O-25**	**NO-21**	**NO-23**	**NO-25**
Fe^{2+}	1.26	1.28	1.41	1.26	1.39	1.42
Dipole moment (D)	5.9	5.6	4.4	3.5	3.7	4.0

bond distances of **2O-14** are shortened by 0.055 and 0.053 Å, respectively, relative to those of **2O-16**. As a more compact structure, **2O-14** should be also more stable than **2O-16**; however, the result is the opposite. The reason is similar to that for the **NO-14**–**NO-16** pairs.

The least stable complexes are **NO-12** and **2O-12**. Comparing their geometries with the corresponding structures of **NO-14(6)** and **2O-14(6)**, we can observe that both of the two doublet state complexes have the shortest chelated bonds between Fe^+ and each corresponding glycine. For **NO-12**, it has lower energy than the corresponding **2O-12** isomer. In comparison with the ground-state **NO-16**, we can observe that the **NO-12** isomer has a smaller dipole moment (2.1 vs 3.4 D). However, the energy calculations show that **NO-12** is 28.9 kcal mol^{-1} in energy higher than **NO-16** one. The reason for this lies in the larger energy gap of their corresponding spin-state metal cations, which makes **NO-12** higher in energy than **NO-16**.

In contrast to the electron configurations of the metal cation in the **2O-12(4)** and the **2O-16** complexes, we can also observe a similar phenomenon to that analyzed above for **NO-12(4)** and the **NO-16**. In addition, the 4s occupation (0.63) of **2O-12** is higher than that (0.47) of the **NO-12** (see Table 5), which confirms reveals the better stability of **NO-12** than **2O-12** from another angle. The larger deformation energy of **2O-12** would destabilize its geometry.

Relative stability and geometries of six glycine–Fe^{2+} isomers

As when dealing with the glycine–Fe^+ isomers, the same optimization schemes were also applied to the Fe^{2+}-chelated glycine complexes. Figure 3 shows the six glycine–Fe^{2+} isomers with different multiplicities. Their relative energies are given in Table 6. They are denoted as **2O-2m** and **NO-2m** (**m** = **1**, **3** or **5**), in which the meanings of **2O** and **NO** are as defined above; the number **2** denotes the valence state of these complexes and **m** stands for the multiplicity, as for **n** above. Table 6 implies that the most stable mode corresponds to the metal ion with a quintet state interacting with the two oxygen ends of zwitterionic glycine, as obtained for the most stable glycine–Cu^{2+} (Ref. 1) and glycine–Zn^{2+} (Refs 2 and 27).

The second most stable mode is **NO-25** also with the quintet state, in which Fe^{2+} is bound to both the amino nitrogen and carbonyl oxygen of glycine, similarly to the **NO-16** in structure. The results show that the energy ordering of these different glycine–Fe^{2+} isomers is very different from that of the glycine–Fe^+ systems, in which the ordering is **NO-16** < **NO-14** < **2O-16** < **2O-14** < **NO-12** < **2O-12**, whereas for glycine–Fe^{2+} the following ordering is observed: **2O-25** < **NO-25** < **NO-23** < **2O-23** < **2O-21** < **NO-21**. That is, the ground state of glycine–Fe^{2+} derives from ionization of the zwitterionic glycine–Fe^+, not from ionization of the neutral glycine–Fe^+(**NO-1n**).

In addition, the marked distinction between the geometry features of **2O-1n** and **2O-2m** isomers is due to the different NH_3 orientations in their corresponding complexes. Turning the tetrahedral NH_3 geometry of **2O-1n** 180° around the C2—N3 bond, we can obtain the corresponding **2O-2m** complex structures. It is noted that H6 in the **2O-1n** isomers has an obvious hydrogen bond effect, e.g. O5···H6 = 1.882 Å in **2O-12**. However, the effects in **2O-2m** disappear owing to the longer contact distance between H6 (in the **NO-2m** isomers) or H9 and H10 (in the **2O-2m** isomers) and the O5 sites of the corresponding complexes, e.g. O5···H10 = 2.727 Å in **2O-25**. They all have C_s-symmetric geometries except for the triplet state ones for these glycine–Fe^{2+} isomers, also different from those C_1-symmetric glycine–Fe^+ complexes.

Table 4. Binding energies (kcal mol^{-1}) and main contributions of glycine–Fe^+ isomers obtained at the BHLYP/basis4//B3LYP/basis1 level[a]

	2O-12	**2O-14**	**2O-16**	**NO-12**	**NO-14**	**NO-16**
ΔE	−50.1	−47.4	−44.5(−43.7)	−67.7	−64.5	−62.4(−61.5)
ΔE_d	28.4	27.1	27.4	7.4	7.1	7.6
ΔE_e	−97.9	−92.9	−89.4	−91.9	−89.3	−79.8

[a] The values in parentheses are corrected by BSSEs.

Table 5. Electron populations of metal ions in the six glycine–Fe^{+} isomers obtained at the B3LYP/basis1 level

	2O-12			**2O-14**			**2O-16**		
	3d	4s	4p	3d	4s	4p	3d	4s	4p
Total	6.56	0.63	0.02	6.34	0.79	0.03	6.00	1.09	0.05
α	3.54	0.55	0.01	4.97	0.10	0.02	4.99	0.97	0.04
β	3.01	0.08	0.01	1.38	0.70	0.01	1.01	0.13	0.01
	NO-12			**NO-14**			**NO-16**		
	3d	4s	4p	3d	4s	4p	3d	4s	4p
Total	6.65	0.47	0.02	6.34	0.77	0.03	6.00	1.07	0.05
α	3.64	0.41	0.01	4.95	0.10	0.02	4.98	0.95	0.04
β	3.01	0.06	0.01	1.39	0.67	0.01	1.02	0.12	0.01

Binding energy and main contributions of glycine–Fe^{+} isomers

Table 4 reports the binding energy (ΔE) and its two main contributions, deformation energy (ΔE_{d}) and electrostatic energy (ΔE_{e}), of the six different glycine–Fe^{+} isomers. Unexpected by, the largest binding energy of $-67.7\,\mathrm{kcal\,mol^{-1}}$ belongs to the **NO-12** isomer. The smallest binding energy ($-44.5\,\mathrm{kcal\,mol^{-1}}$), however, belongs to **2O-16**, the third most stable isomer. The BSSE corrected result shows that the value is $-43.7\,\mathrm{kcal\,mol^{-1}}$. In general, the binding strengths of **NO-1n** isomers are stronger than those of the **2O-1n** counterparts with corresponding multiple states, such as **NO-14** > **2O-14** and **NO-16** > **2O-16**, which are in agreement with the fact that the **NO** mode is preferred to the **2O** mode for these glycine–Fe^{+} isomers. However, the ordering of binding energies of these isomers is almost the reverse of that of their relative energies, and the following discussions focus on this interesting difference.

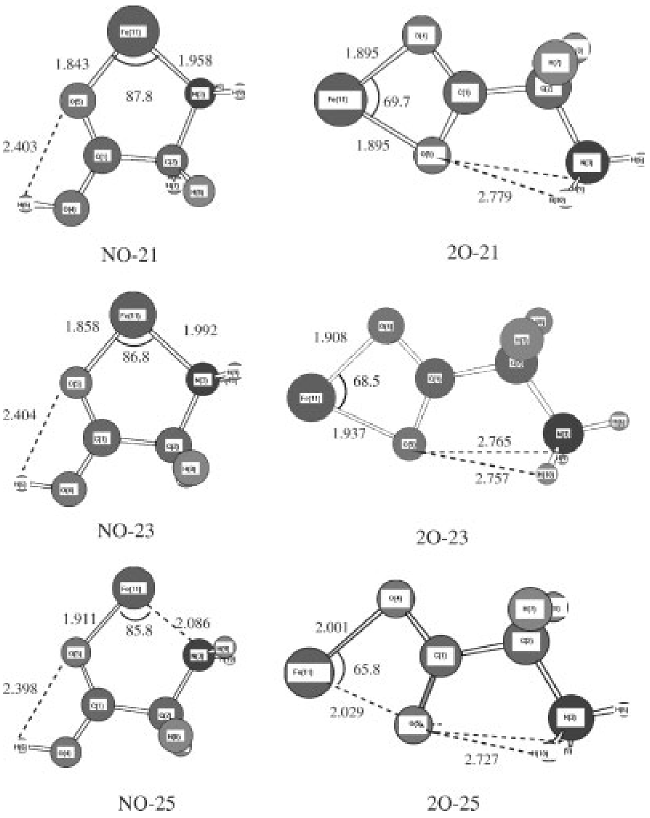

NO-21 2O-21

NO-23 2O-23

NO-25 2O-25

Figure 3. B3LYP/basis1-optimized glycine–Fe^{2+} isomers. Distances in ångstroms and angles in degree

The contributions of the binding energies listed in Table 4 indicate that the binding energies are still electrostatic in origin. For the **2O-1n** isomers, the deformation energy also plays an important role, whereas that in **NO-1n** is smaller.

For **NO-16**, Table 3 shows that the charge-transfer contribution of Fe^{+} is similar to that in **NO-14** (0.35 vs 0.36). **NO-14** readily promotes 4s-3d transition to reduce the repulsion due to its relatively higher 3d population (6.34) and lower 4s population ($0.79 < 1$), whereas **NO-16** mainly reduces the repulsion by 4s4p hybridization. Hence we can conclude that the Pauli repulsion in **NO-16** would be larger than the latter, evidenced by its longer bonding distances. Table 4 shows that the deformation energy contributions for the two different multiple-state complexes are almost in identical (7.1 vs $7.6\,\mathrm{kcal\,mol^{-1}}$). In addition, the lower electrostatic contribution ($-79.8\,\mathrm{kcal\,mol^{-1}}$) of **NO-16** [relative to that of **NO-14** ($-89.3\,\mathrm{kcal\,mol^{-1}}$)] also makes **NO-16** have a lower binding strength. The $3.7\,\mathrm{kcal\,mol^{-1}}$ [$5.8\,\mathrm{kcal\,mol^{-1}}$ (Refs 9 and 10)] ^{4}F–^{6}D atomic (Fe^{+}) separation, however, makes it more stable. In summary, the stronger electrostatic and polarized effects and less Pauli repulsion and deformation of **NO-14** favor its binding strength. However, the more stable metal cation (^{6}D) in **NO-16** makes it more stable than **NO-14**.

In comparison with the five contributions of the binding energies of the lower spin **NO-12** and **NO-14**, we can observe that both complexes have almost the same deformation energies (7.4 vs $7.1\,\mathrm{kcal\,mol^{-1}}$). The lower spin complex shows a stronger electrostatic energy ($-91.9\,\mathrm{kcal\,mol^{-1}}$) and shorter bonding distances owing

Table 6. Relative energies (kcal mol^{-1}) of glycine–Fe^{2+} isomers obtained at the different levels[a]

Level	**2O-25**	**NO-25**	**2O-23**	**NO-23**	**2O-21**	**NO-21**
B3LYP/basis1	0.0(53.4)	4.3(52.4)	22.4(52.8)	29.5(52.3)	40.9(52.9)	62.2(52.6)
B3LYP/basis2//B3LYP/basis1	0.0	5.5	19.9	28.3	60.7	58.3
B3LYP/basis3//B3LYP/basis1	0.0	4.8	20.1	21.8	61.3	58.1
BHLYP/basis4//B3LYP/basis1	0.0	2.3	63.1	48.4	76.1	78.7

[a] The values in parentheses are the ZPVEs of the corresponding complexes. The results in the rows 3 and 4 are corrected with the unscaled ZPVEs.

to less Pauli repulsion, evidenced by its greater 4s (0.47, see Table 5) electron promotion to the 3d orbital[10] (6.65) relative to those (4s 0.77, 3d 6.34) in the **NO-14** complex. The slightly greater charge transfer (0.37 vs 0.36) of the lower spin metal cation listed in Table 3 also favors the binding of **NO-12**. Hence, its binding strength is stronger than that of **NO-14**. However, **NO-14** is also more stable than **NO-12** in energy. The origin of this can also be attributed to the significantly greater atomic energy separation (^{2}G–^{4}F = 34.0 kcal mol^{-1}) between the two different multiple-state metal cations, i.e. all the energy lowering resulting from the metal–ligand coupling cannot compensate for the loss of the energy enhancement of the metal cation. Hence the compositive effects give the lower spin **NO-12** isomer hold a stronger binding strength but poorer stability.

A similar comparison can be made between the **NO-12** and **NO-16** isomers, and similar comparisons between these different multiple-state **2O-1n** isomers can also be made as above for the **NO-1n** isomers.

Now we discuss the difference between the **NO-1n** complex and the corresponding multiple-state **2O-1n** complexes. Taking the comparison between the most stable **NO-16** and **2O-16** as an example, a comparison with the several contributions in **2O-16** and in **NO-16** reveals that higher electrostatic and polarized energies (-89.4 vs -79.8 kcal mol^{-1}), similar electron transfer (0.30 vs 0.35) and similar electron populations [3d (6.00 vs 6.00), 4s (1.09 vs 1.07), 4p (0.05 vs 0.05)] will be favorable to the binding of **2O-16**. However, the larger deformation effect [27.4 kcal mol^{-1} (**2O**) vs 7.6 kcal mol^{-1} (**NO**)] of **2O-16** would greatly destabilize the complex. Hence the electrostatic energy difference (-9.6 kcal mol^{-1}) canot compensate for the loss of deformation difference (19.8 kcal mol^{-1}) and thus results in a lower binding energy and poorer stability of **2O-16**.

Binding energy and main contributions of glycine–Fe^{2+} isomers

Table 7 gives the binding energies of these divalent iron cation-chelated glycine isomers. The binding energy order is **2O-21** > **NO-21** > **NO-23** > **2O-23** > **2O-25** > **NO-25**, not consistent with their relative energy (absolute value) ordering. In comparison with those of glycine–Fe$^+$ isomers, we find that all the terms in Table 7 are larger than their counterparts in Table 4 for the glycine–Fe$^+$ systems.

In contrast with **2O-23** and the $^5A''$ state **2O-25**, we can observe that the former has a larger deformation energy (46.1 vs 41.5 kcal mol^{-1}), which disfavors the stability of the complex. However, the former also has an electrostatic energy contribution 22.0 kcal mol^{-1} higher than that of the latter and more electron transfer (0.72 vs 0.59, see Table 3), which is advantageous for its binding strength and stability. Table 8 shows that both complexes have similar electron populations in the 4s4p orbital, but different 3d occupancies. Owing to the Fe^{2+} lying in an excited state in **2O-23**, there would be a stronger electrostatic attraction between the 3d holes of the metal ion and the pairs of the two oxygens in the zwitterionic glycine ligand, which favors the combination of **2O-23** relative to the **2O-25**. Natural bonding orbital analysis at the B3LYP/basis1 level shows that **2O-25** belongs to a bidentate complex, in which 89.4% 2p electron of O4 and 10.4% 3d4s electron of the metal cation in the β orbital form the O4—Fe bond, while the hybridization of 90.8% 2p electron of O5 and 9.2% 3d4s electron of Fe^{2+} in the same orbital generates the O5—Fe bond. Owing to the attraction effect of empty 3d orbitals, the **2O-23** complex is also a bidentated one with O5—Fe and O4—Fe bonds formed, respectively, by the hybridization of 87.4% 2p electron of O5 and 12.6% 3d4s electron of Fe^{2+} and by hybridization of 85.5% 2p electron of O4 and 14.5% 3d4s electron in the α orbital. We can observe that there are more components of Fe cation participating in the bonding in the **2O-23** complex. Hence both the O5—Fe and O4—Fe bonds in **2O-23** are shorter than those in **2O-25**. All these factors indicate that **2O-23** should have a binding energy similar to or even larger than that of **2O-25**. However, the considerable energy gap (41.9 kcal mol^{-1}) between the triplet and the quintet state metal cations also cannot be compensated by all the

Table 7. BSSE-corrected binding energies (kcal mol^{-1}) and main contributions of glycine–Fe^{2+} isomers obtained at the BHLYP/basis4//B3LYP/basis1 level

	2O-21	**2O-23**	**2O-25**	**NO-21**	**NO-23**	**NO-25**
ΔE	-228.1	-179.3	-178.4	-225.6	-195.1	-175.0
ΔE_d	46.8	46.1	41.5	17.2	16.0	13.9
ΔE_e	-328.2	-324.2	-302.2	-320.3	-312.7	-292.1

Table 8. Electron populations of metal ions in the six glycine–Fe^{2+} isomers obtained at the B3LYP/basis1 level

	2O-21			**2O-23**			**2O-25**		
	3d	4s	4p	3d	4s	4p	3d	4s	4p
Total	6.30	0.19	0.01	6.33	0.15	0.01	6.15	0.17	0.02
α				4.17	0.10	0.01	4.98	0.10	0.01
β				2.16	0.05		1.18	0.06	
	NO-21			**NO-23**			**NO-25**		
	3d	4s	4p	3d	4s	4p	3d	4s	4p
Total	6.36	0.10	0.01	6.28	0.15	0.01	6.15	0.17	0.02
α				4.14	0.10	0.01	4.98	0.10	0.01
β				2.14	0.06	0.01	1.18	0.06	

favorable factors mentioned above and results in a poorer stability of **2O-23** relative to **2O-25**.

The C_s-symmetric **2O-21** ($^1A'$) has more 3d holes than **2O-23**. These holes will have a stronger attraction to the lone electron pairs of the two oxygens of the glycine ligand. Hence it has shorter O4—Fe and O5—Fe bonds than those in **2O-23**. Compared with **2O-23**, **2O-21** has a higher electrostatic energy (−328.2 vs −324.2 kcal mol^{-1}), a slightly greater electron transfer (0.74 vs 0.72) contribution and a similar deformation energy (46.8 vs 46.1 kcal mol^{-1}), which favor its stability. Although the less 3d4s mixing can increase the Pauli repulsion, **2O-21** should still have a stronger binding strength. Its poorer stability relative to **2O-23** also stems from the larger energy gap (54.8 kcal mol^{-1}) between the singlet state metal cation and the triplet state cation.

Similar comparisons can also be made for the different multiple-state **NO-2m** isomers.

For the C_s-symmetric **2O-25** and C_s-symmetric **NO-25**, analysis indicates that the former has more electrostatic and polarized energy and equivalent 3d4s4p electron population and electron transfer but a larger deformation energy relative to the latter. Hence we can also mainly ascribe the larger binding energy and stronger stability of the former to its stronger electrostatic and polarized effects.

CONCLUSIONS

Studies of several Fe^{+}/Fe^{2+}-chelated glycine complexes with different multiple states have been reported. Each with three kinds of possible multiplicities, the two most stable coordination modes of the metal–glycine ligand were taken into account. The results indicate that the most stable glycine–Fe^{+} isomer is **NO-16**, in which sextet state Fe^{+} is bound to both amino nitrogen and carbonyl oxygen, and it has a binding energy of −61.5 kcal mol^{-1}. The binding and relative energies indicate that those complexes with less spin states would have larger binding strength' owing to the greater electrostatic and polarized contributions but poorer stability relative to those with higher spin state owing to the larger metal atomic energy gap. Compared with the **NO-1n** isomers, the **2O-1n** isomers have poorer stability. For the glycine–Fe^{2+} isomers, the ground-state structure is very different from that of glycine–Fe^{+}, derived from the interaction of the quintet state metal cation with the ends of two oxygens of the C_s-symmetric zwitterionic glycine with the binding energy of −178.4 kcal mol^{-1}. The relative energies of these complexes increase with the reduction of the corresponding multiplicity. In contrast to the ordering of the monovalent glycine–Fe^{+} complexes, the divalent metal ion-chelated glycine complexes prefer the **2O** combination mode to the corresponding multiple-state **NO** mode.

The binding energy analysis implies that the electrostatic effect plays a dominant role in the glycine–Fe^{+} combination, and also affects the deformation of the glycine moiety in these different complexes. The origin of the binding energy differences among the different multiple-state glycine–Fe^{+} isomers but with the same combination mode mainly lies in the different electrostatic and polarized effects. For the glycine–Fe^{+} isomers with two different combination modes but same multiple states, the difference in binding strength mainly stems from the different deformation effects. For the glycine–Fe^{+} complexes with same combination mode but different multiple states, the higher the multiple state is, the lower is the binding energy but the stronger the stability. This phenomenon arises because the greater electrostatic contribution of the lower spin complex cannot compensate for the loss of energy enhancement of its corresponding metal cation relative to that of the higher spin counterpart. The same applies to the glycine–Fe^{2+} isomers, but these have higher deformation energies resulting from their larger electrostatic and polarized effects relative to those glycine–Fe^{+} isomers.

A suitable method followed by larger and suitable basis sets for the energy calculations of these more unpaired-electron glycine–Fe^{+}/Fe^{2+} systems are indispensable, otherwise a larger error would occur and even a wrong conclusion could be drawn. By comparisons and compositive considerations regarding both the accuracy and computation cost, the BHLYP/basis4 method is relatively ideal, although it underestimates the energies of the systems to some extent.

Acknowledgments

This work was supported by the National Natural Science Foundation of China (20273040) and the Natural Science Foundation of Shandong Province (Key Project Z2003B01). The support from SRFDP is also acknowledged.

REFERENCES

1. Bertran J, Rodriguez-Santiago L, Sodupe M. *J. Phys. Chem. B* 1999; **103**: 2310–2317.
2. Rogalewicz F, Ohanessian G, Gresh N. *J. Comput. Chem.* 2000; **21**: 963–973.
3. Hoyau S, Ohanessian G. *J. Am. Chem. Soc.* 1997; **119**: 2016–2024.
4. Remko M, Rode BM. *Chem. Phys. Lett.* 2000; **316**: 489–494.
5. Marino T, Russo N, Toscano M. *J. Inorg. Biochem.* 2000; **79**: 179–185.
6. Rodriguez-Santiago L, Sodupe M, Tortajada J. *J. Phys. Chem. A* 2001; **105**: 5340–5347.
7. Shoeib T, Rodriquez CF, Siu M, Hopkinson AC. *Phys. Chem. Chem. Phys.* 2001; **3**: 853.
8. Rulisek L, Havlas Z. *J. Am. Chem. Soc.* 2000; **122**: 10428–10439.
9. Rosi M, Bauschlicher CW Jr. *J. Chem. Phys.* 1989; **90**: 7264.
10. Langboff SR, Bauschlicher CW Jr, Partridge H, Sodupe M. *J. Phys. Chem.* 1991; **95**: 10677.
11. Hoyau S, Pélicier J-P, Rogalewicz F, Hoppilliard Y, Ohanessian G. *Eur. J. Mass Spectrom.* 2001; **7**: 303.
12. Becke AD. *J. Chem. Phys.* 1993; **98**: 5648.
13. Lee C, Yang W, Parr RG. *Phys. Rev. B* 1988; **37**: 785.
14. Leji F, Adamo C, Barone V. *Chem. Phys. Lett.* 1994; **230**: 189.
15. Barone V, Adamo C, Leji F. *J. Chem. Phys.* 1995; **102**: 364.
16. Stepanian SG, Reva ID, Radchenko ED, Rosado MTS, Duarte MLTS, Fausto R, Adamowicz L. *J. Phys. Chem. A* 1998; **102**: 1041–1054; Stepanian SG, Reva ID, Radchenko ED, Adamowicz L. *J. Phys. Chem.* A 1998; **102**: 4623–4629.
17. (a) Møller C, Plesset MS. *Phys. Rev.* 1934; **46**: 618; (b) Head-Gordon M, Pople JA, Frisch MJ. *Chem. Phys. Lett.* 1988; **153**: 503; (c) Frisch MJ, Head-Gordon M, Pople JA. *Chem. Phys. Lett.* 1990; **166**: 275; (d) Saebo S, Almlof J. *Chem. Phys. Lett.* 1989; **154**: 83.
18. (a) Petersson GA, Al-Laham MA. *J. Chem. Phys.* 1991; **94**: 6081; (b) Petersson GA, Bennett A, Tensfeldt TG, Al-Laham MA, Shirley WA, Mantzaris J. *J. Chem. Phys.* 1988; **89**: 2193.
19. (a) Clark T, Chandrasekhar J, Spitznagel GW, Schleyer PvR. *J. Comput. Chem.* 1983; **4**: 294; (b) Frisch MJ, Pople JA, Binkley JS. *J. Chem. Phys.* 1984; **80**: 3265.
20. Raghavachari K, Trucks GW. *J. Chem. Phys.* 1989; **91**: 1062.
21. Baerends EJ, Branchadell V, Sodupe M. *Chem. Phys. Lett.* 1997; **265**: 481.
22. (a) Cizek J. *Adv. Chem. Phys.* 1969; **14**: 35; (b) Purvis GD, Bartlett RJ. *J. Chem. Phys.* 1982; **76**: 1910; (c) Scuseria GE, Janssen CL, Schaefer HF III. *J. Chem. Phys.* 1988; **89**: 7382; (d) Scuseria GE, Schaefer HF III. *J. Chem. Phys.* 1989; **90**: 3700; (e) Pople JA, Head-Gordon M, Raghavachari K. *J. Chem. Phys.* 1987; **87**: 5968.
23. Becke AD. *J. Chem. Phys.* 1993; **98**: 1372.
24. Rodriguez-Santiago L, Sodupe M, Oliva A, Bertran J. *J. Phys. Chem. A* 2000; **104**: 1256.
25. Boys SF, Bermardi F. *Mol. Phys.* 1970; **19**: 553.
26. Strittmatter EF, Lemoff AS, Williams ER. *J. Phys. Chem. A* 2000; **104**: 9793.
27. Kitaura K, Morokuma K. *Int. J. Quantum Chem.* 1976; **10**: 325.
28. Glendening ED, Streitwieser A. *J. Chem. Phys.* 1994; **100**: 2900.
29. Frisch MJ, Trucks GW, Schlegel HB, Scuseria GE, Robb MA, Cheeseman JR, Zakrzewski VG, Montgomery JA Jr, Stratmann RE, Burant JC, Dapprich S, Millam JM, Daniels AD, Kudin KN, Strain MC, Farkas O, Tomasi J, Barone V, Cossi M, Cammi R, Mennucci B, Pomelli C, Adamo C, Clifford S, Ochterski J, Petersson GA, Ayala PY, Cui Q, Morokuma K, Malick DK, Rabuck AD, Raghavachari K, Foresman JB, Cioslowski J, Ortiz JV, Baboul AG, Stefanov BB, Liu G, Liashenko A, Piskorz P, Komaromi I, Gomperts R, Martin RL, Fox DJ, Keith T, Al-Laham MA, Peng CY, Nanayakkara A, Challacombe M, Gill PMW, Johnson B, Chen W, Wong MW, Andres JL, Gonzalez C, Head-Gordon M, Replogle ES, Pople JA. *Gaussian 98, Revision A.9.* Gaussian: Pittsburgh, PA, 1998.
30. Ai H, Bu Y, Han K. *J. Chem. Phys.* 2003; **118**: 10973.
31. Chase MW Jr, Davies CA, Downey JR Jr, Frurip DJ, McDonald RA, Syverud AN. *J. Phys. Chem. Ref. Data* 1985; **14**(Suppl. 1).